SLAC-PUB-5130
CALT-68-1606
December 1989
T/E

Resonant Substructure in $K^-\pi^+\pi^+\pi^-$ Decays of D^0 Mesons[†]

J. Adler, Z. Bai, G.T. Blaylock, T. Bolton, J.-C. Brient, T.E. Browder, J.S. Brown, K.O. Bunnell, M. Burchell, T.H. Burnett, R.E. Cassell, D. Coffman, V. Cook, D.H. Coward, F. DeJongh, D.E. Dorfan, J. Drinkard, G.P. Dubois, G. Eigen, K.F. Einsweiler, B.I. Eisenstein, T. Freese, C. Gatto, G. Gladding, C. Grab, J. Hauser, C.A. Heusch, D.G. Hitlin, J.M. Izen, P.C. Kim, L. Köpke, J. Labs, A. Li, W.S. Lockman, U. Mallik, C.G. Matthews, A.I. Mincer, R. Mir, P.M. Mockett, B. Nemati, A. Odian, L. Parrish, R. Partridge, D. Pitman, S.A. Plaetzer, J.D. Richman, H.F.W. Sadrozinski, M. Scarlatella, T.L. Schalk, R.H. Schindler, A. Seiden, C. Simopoulos, A.L. Spadafora, I.E. Stockdale, W. Stockhausen, W. Toki, B. Tripsas, F. Villa, M.Z. Wang, S. Wasserbaech, A. Wattenberg, A.J. Weinstein, S. Weseler, H.J. Willutzki, D. Wisinski, W.J. Wisniewski, R. Xu, Y. Zhu

The Mark III Collaboration

California Institute of Technology, Pasadena, CA 91125
University of California at Santa Cruz, Santa Cruz, CA 95064
University of Illinois at Urbana-Champaign, Urbana, IL 61801
University of Iowa, Iowa City, IA 52242
Stanford Linear Accelerator Center, Stanford, CA 94309
University of Washington, Seattle, WA 98195

Abstract

We determine the resonant substructure of $D^0 \to K^-\pi^+\pi^+\pi^-$ decays using a five-dimensional maximum likelihood technique to extract the relative fractions and phases of the amplitudes contributing to this final state. We find that two-body decay modes account for at least 76% of all decays. We obtain branching ratios for several decay modes including $\mathrm{B}(D^0 \to K^- a_1^+) = 9.0 \pm 0.9 \pm 1.7\%$, $\mathrm{B}(D^0 \to \overline{K}^{*0}\rho^0) = 1.9 \pm 0.3 \pm 0.7\%$, and $\mathrm{B}(D^0 \to K_1(1270)^-\pi^+) = 1.8 \pm 0.5 \pm 0.8\%$. For the decay mode $D^0 \to \overline{K}^{*0}\rho^0$, the $\overline{K}^{*0}$ and ρ^0 are found to be polarized with their spins oriented in the direction of their motion as seen from the D^0 frame.

Submitted to *Physical Review Letters*

[†] This work was supported in part by the U.S. Department of Energy, under contracts DE-AC03-76SF00515, DE-AC02-76ER01195, DE-AC02-87ER40318, DE-AC03-81ER40050, DE-AM03-76SF0034, and by the National Science Foundation.

Theoretical predictions for exclusive hadronic D decays have been limited to two-body decay modes.[1] Comparison of these predictions with data must in general be made by measuring the resonant substructure of multibody final states. For example, the branching ratios for the $D \to \overline{K}\rho$ and $D \to \overline{K}^*\pi$ decay modes have been obtained by measuring the resonant substructure of $\overline{K}\pi\pi$ final states.[2-5] In order to study two-body decay modes such as those to two vector mesons (VV) and to a pseudoscalar and an axial vector meson (PA), we have extended the analysis to higher multiplicity final states. The Mark III data sample contains a large number of reconstructed events in several $\overline{K}\pi\pi\pi$ final states. We present herein an analysis of the resonant substructure of the $K^-\pi^+\pi^+\pi^-$ final state[6] which shows that two-body decays are the principal component; we also obtain branching ratios of VV, PA, and nonresonant decay modes.

The data were collected near the peak of the $\psi(3770)$ with the Mark III detector[7] at the SLAC e^+e^- storage ring SPEAR. We select candidate $D^0 \to K^-\pi^+\pi^+\pi^-$ events using the procedure described in an earlier analysis of D meson branching fractions.[8] Each $K^-\pi^+\pi^+\pi^-$ combination is kinematically constrained to the D^0 mass, with the recoil mass allowed to vary. Since D mesons are produced in pairs in the decay of the $\psi(3770)$, the signal can be seen in the recoil mass plot as a peak at the D^0 mass, as shown in Fig. 1. There are 1281 ± 45 events in the peak. With this type of constraint, the kinematical limits of phase space are the same for all events throughout the recoil mass plot, and the resonant substructure of the background can be directly determined using all events outside the signal region.

We perform an unbinned maximum likelihood fit to determine the contribution

of each decay mode to the $K^-\pi^+\pi^+\pi^-$ final state. The likelihood function $\mathcal{L}$, consisting of a signal term $\mathcal{L}_S$ and a background term $\mathcal{L}_B$, is a function in the five-dimensional phase space defined by the four-momenta of the decay products of the D candidate:

$$\mathcal{L} = \frac{R\mathcal{L}_S + \mathcal{L}_B}{R+1}. \tag{1}$$

For each event we calculate the ratio of signal to background, R, as a function of recoil mass.

The function $\mathcal{L}_S$ is a coherent sum of complex amplitudes S_j whose relative fractions f_j and phases α_j are allowed to vary:

$$\mathcal{L}_S = \epsilon\,\phi\,|\sum_j \sqrt{f_j}\; e^{i\alpha_j} S_j|^2. \tag{2}$$

The efficiency function ϵ, the four-body phase space function ϕ, and the symmetrized amplitudes S_j are functions of position in the five-dimensional phase space. The amplitudes S_j consist of a relativistic Breit-Wigner propagator for each resonance in the decay chain, multiplied by a matrix element which depends on the spin and parity of the intermediate resonances and final decay products.

The function $\mathcal{L}_B$ is an incoherent sum of background functions B_j whose relative fractions g_j are allowed to vary:

$$\mathcal{L}_B = \epsilon\,\phi \sum_j g_j B_j. \tag{3}$$

The background is adequately described by a set of functions which model the $\overline{K}^{*0}$, ρ^0 and nonresonant content of the events oustide the signal region.

The fit is performed by minimizing $-\Sigma \ln \mathcal{L}$, where the summation is over all events in the recoil mass plot, after factoring out ϵ and ϕ, which do not depend on the variables in the fit. We calculate ϵ and ϕ using Monte Carlo techniques when

normalizing the B_j, $\mathcal{L}_S$, and $\mathcal{L}_B$, and when making one-dimensional projections of $\mathcal{L}$.

A very large number of decay modes can contribute to the $K^-\pi^+\pi^+\pi^-$ final state; it is not practical to perform a fit that includes all possible decay modes simultaneously. Instead, we perform a number of fits assuming different combinations of partial waves and two-body modes. Only the lowest available partial waves yield significant contributions, and the fractions of two-body amplitudes and the four-body nonresonant amplitude remain consistent in the best fits. Nonresonant $\overline{K}^{*0}\pi^+\pi^-$ and $K^-\rho^0\pi^+$ amplitudes also contribute. The fits are not sensitive to the partial wave content of these three-body amplitudes.

Since the a_1 meson is very broad, the $K^-a_1^+$ amplitude is difficult to distinguish from nonresonant $K^-\rho^0\pi^+$ in which the ρ^0 and π^+ are in a relative S-wave. Fits in which both of these amplitudes are included do not result in a significantly better likelihood; however, the fractions for each of these two amplitudes become highly uncertain, although their combined fraction remains well determined. Fits in which the $K^-a_1^+$ amplitude is replaced by the three-body amplitude result in a significantly poorer fit, with a difference in $-\Sigma \ln \mathcal{L}$ between 12 and 30, depending on the parameters of the fit. Therefore, it is assumed that this particular three-body amplitude does not contribute to the final state studied here.

In the final fit, we include amplitudes for $K^-a_1^+$ and $K_1(1270)^-\pi^+$ decays, an amplitude for S-wave $\overline{K}^{*0}\rho^0$ decays in which the $\overline{K}^{*0}$ and ρ^0 are transversely polarized as seen from the D^0 rest frame, an amplitude for four-body nonresonant decays, an amplitude for $\overline{K}^{*0}\pi^+\pi^-$ decays in which the $\overline{K}^{*0}\pi^-$ system is in a pseudoscalar state, and an amplitude for $K^-\rho^0\pi^+$ decays in which the $K^-\rho^0$ system

is in an axial vector state. We assume 1.26 GeV/c^2 for the mass of the a_1^+, and 0.4 GeV/c^2 for the width.[11] The results of the fit are shown in Table I. The fractions have been scaled so that the likelihood function is properly normalized; due to interference, the fractions do not sum to one. The systematic errors on the fractions are estimated by varying the partial waves of the three-body amplitudes, the event selection criteria, the background parametrization, the parametrizations of the amplitudes, the parameters of the intermediate resonances, and the detector resolution. Table II contains upper limits for the branching ratios of several decay modes which do not yield significant contributions to this final state. These limits represent conservative estimates of the 90% C.L. based on the variations of the fractions in fits with different combinations of amplitudes.

Projections of $\mathcal{L}$ from this fit onto one-dimensional mass plots are shown in Fig. 2. The $\pi^+\pi^-$ combination with the higher mass is referred to as $(\pi^+\pi^-)_{\rm high}$, the other as $(\pi^+\pi^-)_{\rm low}$. The $K^-\pi^+$ combination formed with the π^+ not used in $(\pi^+\pi^-)_{\rm high}$ is referred to as $(K^-\pi^+)_1$, the other as $(K^-\pi^+)_2$. Clear $\overline{K}^{*0}$ and ρ^0 peaks, reproduced well by the fit, are visible. A peak at the $K_1(1270)$ mass is visible in the $K^-(\pi^+\pi^-)_{\rm low}$ mass plot, and is reproduced with an amplitude modeling the three largest decay modes of the $K_1(1270)$. The enhancement at low $K^-\pi^-$ mass is produced by the longitudinal polarization of the a_1 in the $K^-a_1^+$ amplitude, as illustrated in Fig. 3. The presence of the transverse $\overline{K}^{*0}\rho^0$ amplitude leads to angular correlations between $\overline{K}^{*0}$ and ρ^0 decays, as seen in Fig. 4.

Previous analyses of $D^0 \to K^-\pi^+\pi^+\pi^-$ decays[12–15] were incomplete in that the resonant substructure was measured by fitting one-dimensional mass plots to obtain the fraction of $\overline{K}^{*0}\rho^0$, inclusive $\overline{K}^{*0}$, inclusive ρ^0, and nonresonant four-

body contributions. The advantage of the approach used here is that the amplitudes provide a complete description of the decay modes in the five-dimensional phase space and all the information available in the event is used in the fit, making it possible to fit to a general set of amplitudes, *including interference*, to obtain fractions for exclusive decay modes. A comparison with results from other experiments is shown in Table III. We calculate the total $\overline{K}^{*0}$ and ρ^0 content from our fits by summing the appropriate exclusive fractions and taking into account interference between the decay modes. From a similar calculation, we find that the total fraction of the two-body amplitudes is 76%. The total contribution from two-body decay modes could be larger, because the nonresonant amplitudes may contain decays involving broad resonances or tails of resonances above threshold.

The model of Bauer, Stech, and Wirbel, which assumes factorization, has been used to make predictions[16] for VV and PA decays of D mesons. In this model, the branching fractions are $B(D^0 \to \overline{K}^{*0}\rho^0) = 2.5\%$ and $B(D^0 \to K^- a_1^+) = 5.0\%$. We find $B(D^0 \to \overline{K}^{*0}\rho^0) = 1.9 \pm 0.3 \pm 0.7\%$ and $B(D^0 \to K^- a_1^+) = 9.0 \pm 0.9 \pm 1.7\%$, consistent with the predictions. Our results for $D^0 \to \overline{K}^{*0}\rho^0$ are consistent with complete transverse polarization.

We gratefully acknowledge the dedicated efforts of the SPEAR staff. One of us (C.G.) wishes to thank the Fondazione A. Della Riccia for support. This work was supported by the Department of Energy, under contracts DE-AC03-76SF00515, DE-AC02-76ER01195, DE-AC03-81ER40050, DE-AC02-87ER40318, DE-AM03-76SF00034 and by the National Science Foundation.

REFERENCES

1. For a review, see M.A. Shifman, Int. J. Mod. Phys. A **3**, 2769 (1988).

2. R.H. Schindler *et al.*, Phys. Rev. **D24**, 78 (1981).

3. D.J. Summers *et al.*, Phys. Rev. Lett. **52**, 410 (1984).

4. J. Adler *et al.*, Phys. Lett. **196B**, 107 (1987).

5. J.C. Anjos *et al.*, Phys. Rev. Lett. **60**, 897 (1988).

6. We adopt the convention that reference to a state implies reference to its charge conjugate.

7. D. Bernstein *et al.*, Nucl. Instrum. Methods **226**, 301 (1984).

8. R.M. Baltrusaitis *et al.*, Phys. Rev. Lett. **56**, 2140 (1986).

9. J. Adler *et al.*, Phys. Rev. Lett. **60**, 89 (1988).

10. Branching ratios were calculated using $\mathrm{B}(D^0 \to K^-\pi^+\pi^+\pi^-) = 9.1 \pm 0.8 \pm 0.8\%$ from Ref. 9, and the branching ratios of the intermediate resonances to the $K^-\pi^+\pi^+\pi^-$ final state.

11. M. G. Bowler, Phys. Lett. B, **209**, 99 (1988).

12. M. Piccolo *et al.*, Phys. Lett. **70B**, 260 (1977).

13. R. Bailey *et al.*, Phys. Lett. **132B**, 237 (1983).

14. P. Kim, Ph.D. thesis, University of Toronto, 1987 (unpublished).

15. J.C. Anjos *et al.*, contributed paper, International Conference on High Energy Physics, Munich, 1988.

16. M. Bauer, B. Stech, and M. Wirbel, Z. Phys. C **34**, 103 (1987). The prediction for $B(D^0 \to K^- a_1^+)$ is from a private communication with B. Stech.

Table I. Results for $D^0 \to K^-\pi^+\pi^+\pi^-$

Amplitude	Fraction f_j	Phase α_j	Branching Ratio (%)[a]
4-Body Nonresonant	$0.242 \pm 0.025 \pm 0.06$	-1.07 ± 0.08	$2.2 \pm 0.3 \pm 0.6$
$\overline{K}^{*0}\rho^0$ Transverse (S-wave)	$0.142 \pm 0.016 \pm 0.05$	-1.39 ± 0.09	$1.9 \pm 0.3 \pm 0.7$
$K^-a_1(1260)^+$	$0.492 \pm 0.024 \pm 0.08$	0.0	$9.0 \pm 0.9 \pm 1.7$
$K_1(1270)^-\pi^+$	$0.066 \pm 0.019 \pm 0.03$	0.71 ± 0.25	$1.8 \pm 0.5 \pm 0.8$
$\overline{K}^{*0}\pi^+\pi^-$	$0.140 \pm 0.018 \pm 0.04$	3.07 ± 0.09	$1.9 \pm 0.3 \pm 0.6$
$K^-\rho^0\pi^+$	$0.084 \pm 0.022 \pm 0.04$	-0.30 ± 0.13	$0.8 \pm 0.2 \pm 0.4$

[a] Reference 10.

Table II. Upper limits for $D^0 \to K^-\pi^+\pi^+\pi^-$

Amplitude	Branching Ratio (%)[a]
$\overline{K}^{*0}\rho^0$ Longitudinal (S-wave)	< 0.3
$\overline{K}^{*0}\rho^0$ (P-wave)	< 0.3
$K^-a_2(1320)^+$	< 0.6
$K^*(1415)^-\pi^+$	< 1.2
$K_1(1400)^-\pi^+$	< 1.2

[a] Reference 10.

Table III. Fractions of the $K^-\pi^+\pi^+\pi^-$ final state as observed by different experiments

Channel	Mark III	SLAC-LBL[a]	ACCMOR[b]	ARGUS[c]	E691[d]
$\overline{K}^{*0}$ X	$0.207 \pm 0.020 \pm 0.03$			0.39 ± 0.03	$0.26 \pm 0.04 \pm 0.03$
ρ^0 X	$0.855 \pm 0.032 \pm 0.03$			0.86 ± 0.10	$1.06 \pm 0.06 \pm 0.09$
$\overline{K}^{*0}\rho^0$	$0.142 \pm 0.016 \pm 0.05$	$0.1^{+0.11}_{-0.10}$	0.5 ± 0.2	0.35 ± 0.06	
$K^-\rho^0\pi^+$	$0.084 \pm 0.022 \pm 0.04$	$0.85^{+0.11}_{-0.22}$	0.2 ± 0.2	0.51 ± 0.08	
$K^-a_1^+$	$0.492 \pm 0.024 \pm 0.08$			0.51 ± 0.08[e]	
$\overline{K}^{*0}\pi^+\pi^-$	$0.140 \pm 0.018 \pm 0.04$	$0.0^{+0.2}_{-0.0}$	< 0.18	0.04 ± 0.04	
$K^-\pi^+\pi^+\pi^-$	$0.242 \pm 0.025 \pm 0.06$	$0.05^{+0.11}_{-0.05}$		0.11 ± 0.06	

[a] Reference 12. [b] Reference 13. [c] Reference 14. [d] Reference 15.

[e] In the ARGUS analysis, angular distributions of ρ^0 decays outside the $\overline{K}^{*0}$ bands were examined. The $K^-\rho^0\pi^+$ component was found to be consistent with being entirely $K^-a_1^+$.

Figure Captions

1. $D^0 \to K^-\pi^+\pi^+\pi^-$ recoil mass spectrum.

2. Projections of the likelihood function for $D^0 \to K^-\pi^+\pi^+\pi^-$. The solid lines, representing the projections of the likelihood function, are superimposed on histograms of the events in the signal region. The deficit near 0.5 GeV/c^2 in the $(\pi^+\pi^-)_{\rm low}$ mass plot is due to the rejection of $\pi^+\pi^-$ combinations which have a high probability of originating from a K^0_s decay.

3. Qualitative illustration of the $K^-a_1^+$ amplitude. The small vertical arrows indicate the spins of the a_1 and ρ. The relative orbital angular momentum at each vertex is shown. Because of the longitudinal polarization of the a_1 and subsequent polarization of the ρ, the π^- tends to be produced in a forward or backward direction with respect to the direction of the K^-, producing a distribution with an enhancement at low $K^-\pi^-$ mass.

4. Slices of $(K^-\pi^+)_1$ mass vs ϕ, where ϕ is the angle between the $\overline{K}^{*0}$ and ρ^0 decay planes as seen from the D^0 rest frame. In the darkly shaded slice, which contains the $\overline{K}^{*0}$ mass region, an enhancement near ϕ=0 and a larger enhancement near $\phi = \pi$ are visible. The transverse $\overline{K}^{*0}\rho^0$ amplitude is proportional to cos ϕ and accounts for this distribution; the longitudinal $\overline{K}^{*0}\rho^0$ amplitude is constant in ϕ while the P-wave $\overline{K}^{*0}\rho^0$ amplitude is proportional to sin ϕ. Since the sign of the transverse $\overline{K}^{*0}\rho^0$ amplitude reverses from $\phi = 0$ to $\phi = \pi$, there is more constructive interference near $\phi = \pi$.

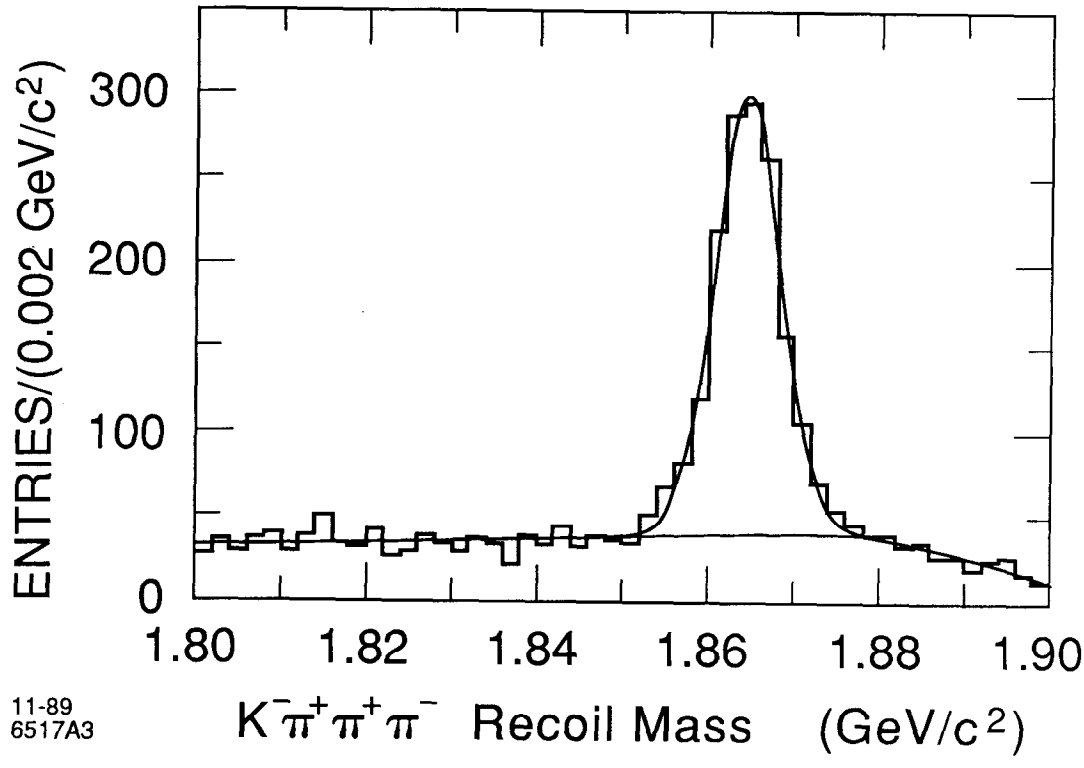
ENTRIES/(0.002 GeV/c²)
300
200
100
0
1.80
1.82
1.84
1.86
1.88
1.90
11-89
6517A3
K⁻π⁺π⁺π⁻ Recoil Mass (GeV/c²)

Fig. 1

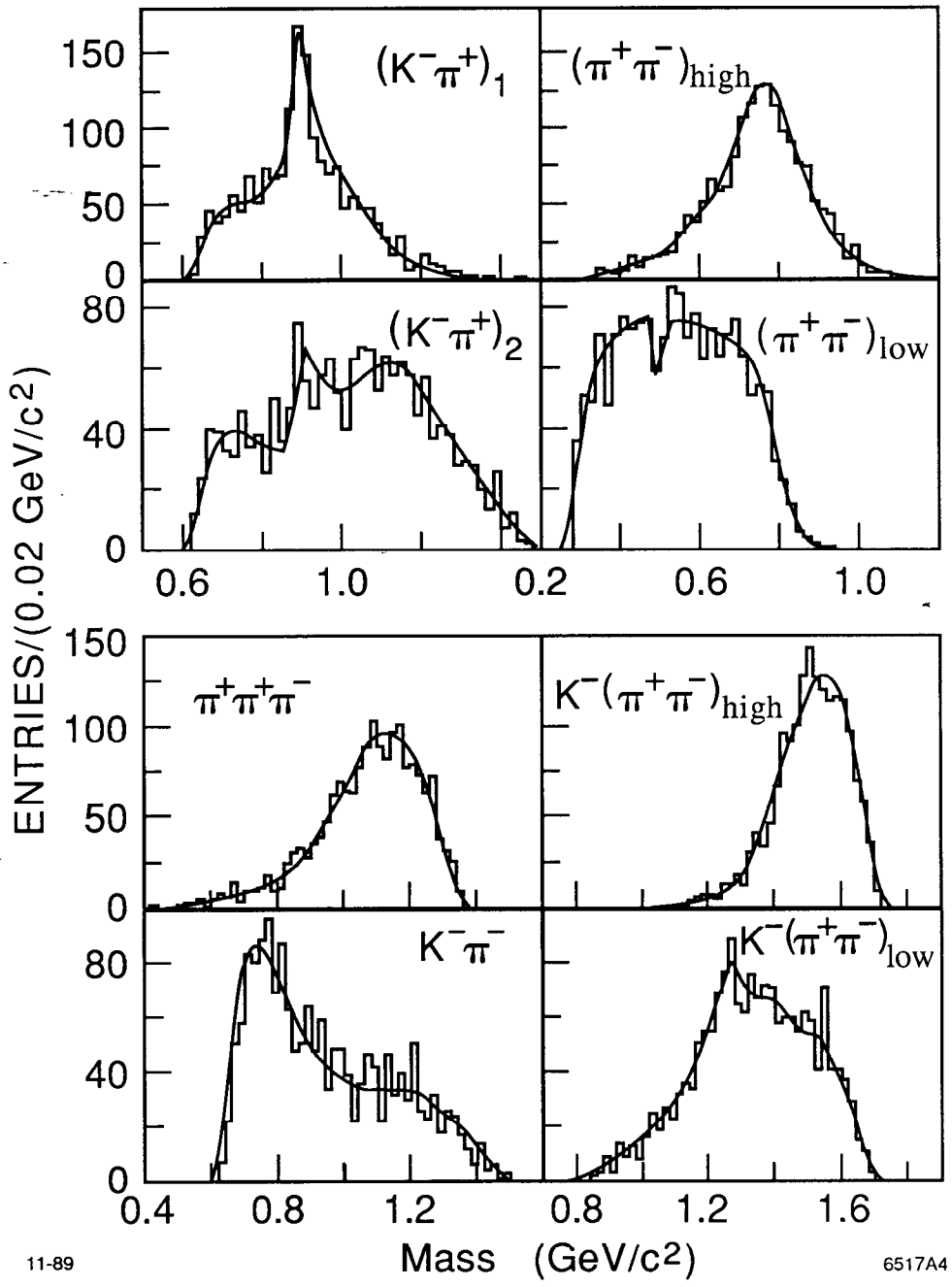
$(K^-\pi^+)_1$
$(\pi^+\pi^-)_{high}$
$(K^-\pi^+)_2$
$(\pi^+\pi^-)_{low}$
$\pi^+\pi^+\pi^-$
$K^-(\pi^+\pi^-)_{high}$
$K^-\pi^-$
$K^-(\pi^+\pi^-)_{low}$
ENTRIES/(0.02 GeV/c²)
Mass (GeV/c²)
11-89
6517A4

Fig. 2

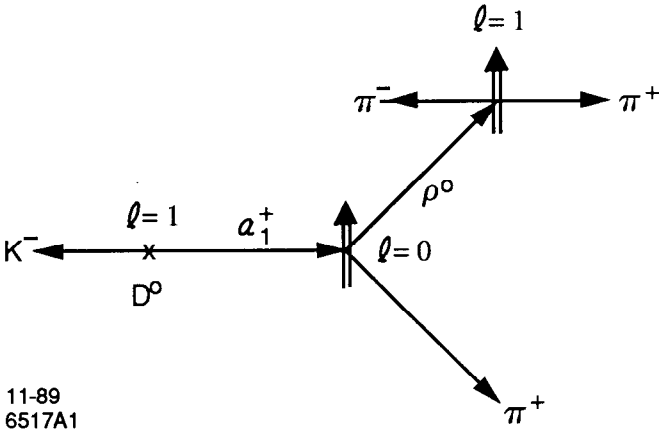

Fig. 3

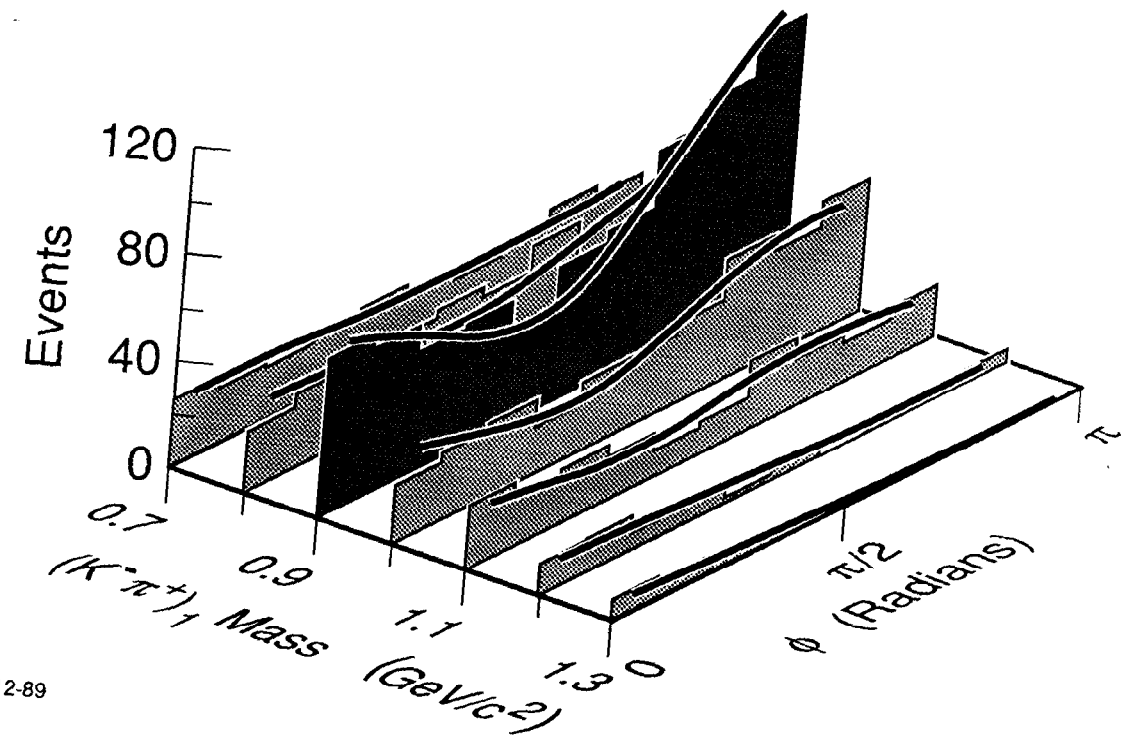
120
80
40
0
Events
0.7
0.9
1.1
1.3
$(K^-\pi^+)_1$ Mass (GeV/c²)
0
π/2
π
Φ (Radians)
12-89
6540A1

Fig. 4